

Weakly Nonlinear Internal Waves in Shear

By Ka-Kit Tung, Denny R. S. Ko, and Jerry J. Chang

An evolution equation in a finite depth fluid for weakly nonlinear long internal waves is derived in a stratified and sheared medium. The equation reduces to the Korteweg-deVries equation when the depth is small compared to the wavelength, and to the Benjamin-Ono equation when the depth is large compared to the wavelength. Both the cases with and without critical levels are investigated. Numerical solutions to the evolution equation are presented to illustrate the effect of shear on the evolution of a waveform.

1. Introduction

It is generally acknowledged that the effects of shear on the internal waves can be divided into two categories: the so-called "kinematic" and "dynamic" effects.

(1) *Kinematic effects* refer to the changes in waveform and wave speed of the internal wave as a result of the shearing action of the background flow.

(2) *Dynamic effects* refer to the possible energy and momentum exchanges between the waves and the background flow, as the shear represents an additional energy source.

The presence and the magnitude of these two effects on internal waves have been investigated by many able researchers in the past. The nature of the effects has been found to depend strongly on the existence of critical layers where the phase speed of the wave equals the speed of the background flow.

In the absence of critical levels, it can be shown that a weakly nonlinear internal wave does not exchange energy and momentum with the background flow. This "noninteraction" theorem is well known; its derivation is briefly sketched for the present case in Appendix A by showing that the background flow does not change in time (to the second order in wave amplitude) in response to the wave momentum and energy fluxes. Therefore, for the case where critical levels do not exist within the flow domain, the effect of the shear on the wave is

Address for correspondence: Professor K. K. Tung, Room 2-332, M.I.T., Cambridge, MA 02139.

STUDIES IN APPLIED MATHEMATICS 65:189-221 (1981)

189

Copyright © 1981 by the Massachusetts Institute of Technology

Published by Elsevier North Holland, Inc.

0022-2526/81/060189+33\$02.50

purely kinematic. This result is further supported by the evolution equation derived in the present paper, which has the same form as in the no shear case, and which possesses wave solutions of permanent form.

When a critical level is present, the effects of shear on the wave depend critically on the relative magnitudes of nonlinearity and viscosity within the critical layer. If viscosity is predominant, energy exchange between the wave and the background flow occurs at the critical layer, the direction of the energy flow being determined by the local Richardson number Ri . When $Ri > \frac{1}{4}$, the results of Booker and Bretherton [6] show that the wave energy is absorbed by the background flow near the critical level. For $Ri < \frac{1}{4}$, the energy flow can go in either direction, depending on Ri and the wavelength of the wave [14].

When nonlinearity is the dominant mechanism in the critical layer, the above results are changed drastically. For the case of an unstratified fluid ($Ri=0$), Benney and Bergeron [5] show that no exchange of energy occurs between the wave and the background flow. As a result normal mode (neutral) eigensolutions exist even in the presence of critical levels.¹ The same conclusion seems to hold for slightly stratified fluids ($|Ri| \ll 1$) [16] and fully stratified flows ($Ri = O(1)$) [20].

The above mentioned analyses also revealed the tendency for the flow within the critical layer to develop sharp shear and thermal boundary layers around the edge of the "cat's-eye" caused by the concentration of vorticity. These regions may be locally unstable when the effects of viscosity are taken into account. Also, there remains the possibility that a nonlinear critical layer may be unstable to secondary instabilities which have not been investigated in this paper.

In the present study, we adopt the assumption that the generated wave under consideration has sufficient amplitude to have a nonlinearly dominated critical layer. To justify this assumption, we show that for most long internal waves in the ocean, the Reynolds number in laminar flows is so large that the effect of viscosity is almost completely overwhelmed by the nonlinearity of the wave. Exceptions to this result may occur if the background flow is highly turbulent. The effect of viscosity is also ignored by assuming that the wave is examined at a time not late enough to permit the effects of viscosity to be felt outside the thin boundary layers within the critical layer (but the time is assumed late enough to permit a quasi-steady-state calculation²). Under these assumptions the background flow does not influence the wave energetically; normal mode solutions can be found even in the presence of critical levels. Thus the results for the case of no critical levels can be carried over to this case and the same evolution equation for the wave amplitude is obtained. Solitary waves are shown to exist as solutions by analogy with the equation for the no shear case.

These qualitative observations are examined using a specific simplified example. It is found that the separations between phase speeds of various modes decrease when the shear is introduced. As the Richardson number is decreased (i.e., shear increases), the wave speeds of all modes are increased, with the lower

¹If such steady states can be reached.

²The evolution of critical layers to steady states has been actively investigated by many authors (e.g., M. Bédard [3], Warn and Warn [24], Stewardson [23], Bédard [4], Brown and Stewartson [8]). The presence of small viscosity seems to be important in the evolution to a steady state by damping out higher harmonics generated by nonlinear interactions, and by preventing the development of sharp gradients inside the critical layer.

wave modes having a slower rate of increase. The lower modes eventually move with the higher modes as the Richardson number is decreased further, until a critical level appears at the location where the background flow speed is a maximum (which is at the boundary in this example). The phase speeds of all modes coalesce at this point. And as the shear is increased further, the critical levels occur in the interior of the flow domain and the higher modes begin to travel *faster* than the lower modes.

The distortion of wave forms by shear can largely be attributed to the change in phase speeds (the eigenvalues) and the vertical distributions (the eigenfunctions). If, say, a mode-2 wave is generated along with some smaller higher modes in the shearless case, the lowest mode (in this case, the mode-2) will travel faster than the higher modes and will emerge as a single "pure" mode after trailing off the higher mode "distortions." When shear is introduced, the separation between the phase speeds is reduced and as a consequence the mode-2 wave and the other higher mode "distortions" tend to travel together for a period of time before breaking up. Visually the combined wave may appear as a distorted mode-2 wave.

By solving the evolution equation numerically, we also studied the evolution of a solitary wave as it propagates into a sheared medium. Three different behaviors are possible, depending on the effect of shear on the nonlinear and dispersive parameters α and β in that equation: (1) the solitary wave steepens and breaks if the nonlinear parameter α becomes larger, (2) the wave disperses if the product βc_0 of the dispersive parameter and linear phase speed decreases, and (3) the waveshape remains unchanged if α and βc_0 are unaltered. In the last case, the waveshape merely speeds up.

Note added: It has come to the present authors' attention that Maslowe and Redekopp recently published an article [22] in which the same subject matter, i.e., solitary internal waves in shear flows, is discussed. The readers are referred to that paper for the derivation of the evolution equation and analytic solutions for the two extreme cases: shallow ($H/l \ll 1$) and deep ($H/l \gg 1$) fluid depths. The present article concerns itself mainly with depths in between these two limits.

2. Derivation of the evolution equation

For the *shearless* case, the evolution equation for a weakly nonlinear internal wave on a thin pycnocline in a finite-depth fluid has been derived by Kubota, Ko, and Dobbs [17]. It is shown there that the equation reduces to the Korteweg-deVries equation in the shallow water limit, and the Benjamin-Ono equation in the deep water limit. The equation has also been shown numerically to possess solitonlike solutions.

The derivation of the corresponding evolution equation for the sheared case is briefly outlined here. For two dimensional flow of an inviscid and incompressible fluid, the governing equations for incompressibility and for horizontal and vertical momentum are

$$\rho_t + \psi_y \rho_x - \psi_x \rho_y = 0, \quad (2.1)$$

$$\rho(\psi_{yt} + \psi_y \psi_{yx} - \psi_x \psi_{yy}) = -p_x, \quad (2.2)$$

$$\rho(\psi_{xt} + \psi_y \psi_{xx} - \psi_x \psi_{xy}) = p_y + \rho g. \quad (2.3)$$

The velocities u and v in the x (horizontal) and y (negative g) directions have been expressed in terms of the streamfunction ψ through

$$u = \psi_y \quad (2.4)$$

and

$$v = -\psi_x. \quad (2.5)$$

We assume that a region (of thickness $O(h)$) of sharp density variation exists within the fluid. This region is called a pycnocline. Outside the pycnocline, stratification may also exist, but the density variation is assumed to be not as sharp as in the pycnocline. The displacement amplitude [$O(a)$] of the wave of interest is small compared to the pycnocline thickness h , and its wavelength is assumed to be large with respect to h ; i.e.,

$$\begin{aligned} \epsilon &\equiv a/h \ll 1, \\ \mu &\equiv h/l \ll 1. \end{aligned} \quad (2.6)$$

The ratio of wavelength l to total fluid depth H is not restricted. The time variation of the wave is taken to be a steady phase propagation plus a slow variation of the amplitude;³ i.e., we assume

$$\frac{\partial}{\partial t} = -c_0 \frac{U_R}{l} \frac{\partial}{\partial \xi} + \frac{U_R}{l} \frac{\partial}{\partial \tau},$$

where

$$l\xi = x - U_R c_0 t$$

and

$$\tau = \epsilon(U_R/l)t,$$

with $U_R \equiv (\Delta\rho/\rho_R)gh$ being a scaling for the phase speed and c_0 being the dimensionless wave speed.

To examine the behavior of the internal wave in the pycnocline, we define an inner variable \tilde{y} as

$$\tilde{y} = y/h.$$

³Doing so, the fast transient behavior of the wave is not considered.

The dependent physical variables in the inner region (i.e., inside the pycnocline) are scaled as follows:

$$\begin{aligned}\rho - \rho_0 &= \varepsilon \Delta \rho \tilde{\rho}(\xi, \tilde{y}, \tau), \\ p - p_0 &= \varepsilon \rho_R U_R^2 \tilde{p}(\xi, \tilde{y}, \tau), \\ \psi - \int^y u_0 dy &= a U_R \tilde{\psi}(\xi, \tilde{y}, \tau),\end{aligned}\tag{2.7}$$

where $u_0 = u_0(y)$ is the background flow velocity in the x -direction, and p_0 and ρ_0 are the background pressure and density field respectively. For the long waves under consideration the background flow is taken to be in hydrostatic balance; i.e.,

$$p_{0y} + \rho_0 g = 0.\tag{2.8}$$

The background variables are nondimensionalized as follows:

$$\begin{aligned}U(\tilde{y}) &= \frac{u_0}{U_R}, \\ \hat{\rho}_0(\tilde{y}) &= \frac{\rho_0}{\rho_R},\end{aligned}$$

and

$$r(\tilde{y}) \equiv -\frac{\rho_{0y}}{\Delta \rho / h} = -\frac{\hat{\rho}_{0y}}{\sigma / h}, \quad \sigma \equiv \frac{\Delta \rho}{\rho_R}.$$

$r(\tilde{y})$ is related to the Brunt-Väisälä frequency N by $N^2 = (\Delta \rho / h) g r / \rho_0$. Note that $r(\tilde{y})$ as defined above is of order 1 irrespective of the order of σ .

The Boussinesq case $\sigma \ll 1$, is first considered. Modifications to the non-Boussinesq case, $\sigma = O(1)$, are examined in Appendix B. Assuming

$$\sigma = O(\varepsilon), \quad \mu = O(\varepsilon)$$

and expanding the inner variables in the following manner:

$$\begin{aligned}\tilde{\psi} &= \tilde{\psi} + \varepsilon \tilde{\psi}_2 + \varepsilon^2 \tilde{\psi}_3 + \dots, \\ \tilde{\rho} &= \tilde{\rho}_1 + \varepsilon \tilde{\rho}_2 + \varepsilon^2 \tilde{\rho}_3 + \dots, \\ \tilde{p} &= \tilde{p}_1 + \varepsilon \tilde{p}_2 + \varepsilon^2 \tilde{p}_3 + \dots,\end{aligned}\tag{2.9}$$

one obtains a hierarchy of perturbation equations; the first two orders in ε give

$$(U - c_0)\tilde{\rho}_{1\xi} + r\tilde{\psi}_{1\xi} = 0,$$

$$(U - c_0)\left[\left(\frac{\partial}{\partial \tilde{y}} - \frac{U_{\tilde{y}}}{U - c_0}\right)\tilde{\psi}_{1\xi}\right] + \tilde{p}_{1\xi} = 0, \quad (2.10)$$

$$\tilde{p}_{1\tilde{y}} + \tilde{\rho}_1 = 0,$$

and

$$(U - c_0)\tilde{\rho}_{2\xi} + r\tilde{\psi}_{2\xi} = -\tilde{\rho}_{1\tau} - [\tilde{\psi}_{1\tilde{y}}\tilde{\rho}_{1\xi} - \tilde{\psi}_{1\xi}\tilde{\rho}_{1\tilde{y}}],$$

$$\begin{aligned} (U - c_0)\left[\left(\frac{\partial}{\partial \tilde{y}} - \frac{U_{\tilde{y}}}{U - c_0}\right)\tilde{\psi}_{2\xi}\right] + \tilde{p}_{2\xi} \\ = -\tilde{\psi}_{1\tilde{y}\tau} - \left(\frac{\sigma}{\varepsilon}\right)\tilde{\rho}_0(U - c_0)\left[\left(\frac{\partial}{\partial \tilde{y}} - \frac{U_{\tilde{y}}}{U - c_0}\right)\tilde{\psi}_{1\tilde{y}}\right] \end{aligned} \quad (2.11)$$

$$- [\tilde{\psi}_{1\tilde{y}}\tilde{\psi}_{1\tilde{y}\xi} - \tilde{\psi}_{1\xi}\tilde{\psi}_{1\tilde{y}\tilde{y}}],$$

with

$$\tilde{p}_{2\tilde{y}} + \tilde{\rho}_2 = 0.$$

In deriving the above sets of equations, it is assumed that $\hat{\rho}_0$ can be written as

$$\hat{\rho}_0 = 1 + \sigma\tilde{\rho}_0(\tilde{y}), \quad \text{where} \quad \tilde{\rho}_0(\tilde{y}) = O(1).$$

The first order equations (2.10) permit the following solutions:

$$\tilde{\psi}_1 = \tilde{A}(\varepsilon, \tau)\phi(\tilde{y}), \quad (2.12)$$

$$\tilde{\rho}_1 = -\frac{r}{U - c_0}\phi\tilde{A}(\varepsilon, \tau), \quad (2.13)$$

and

$$\tilde{p}_1 = -(U - c_0)\left[\frac{\partial}{\partial \tilde{y}} - \frac{U_{\tilde{y}}}{U - c_0}\right]\phi\tilde{A}(\varepsilon, \tau). \quad (2.14)$$

The function ϕ satisfies

$$L\{\phi\} = 0 \quad (2.15)$$

with

$$L \equiv \frac{d^2}{d\bar{y}^2} + \left[\frac{r}{(U-c_0)^2} - \frac{U''}{U-c_0} \right].$$

(Primes denote differentiations with respect to \bar{y} .) This is the Taylor-Goldstein equation for a Boussinesq fluid.

In the absence of critical levels where $U-c_0=0$, there exists ample literature (see e.g. [13]) to show that Equation (2.15) possesses a set of discrete eigenvalues

$$c_0 = c_{0,n}, \quad n = 1, 2, 3, \dots$$

and a corresponding set of eigenfunctions

$$\phi = \phi_n(\bar{y}), \quad n = 1, 2, 3, \dots$$

When critical levels are present in the flow domain, Equation (2.15) becomes singular at where $U(\bar{y})-c_0=0$, and consequently the existence of normal mode solutions to (2.15) of the form assumed has been much in doubt. The critical level problem will be specifically addressed in Section 3. The analyses in the remaining part of this section are based on the assumption of $U-c_0 \neq 0$.

When Equations (2.12)–(2.14) are substituted into (2.11), the second order equations give

$$(U-c_0)L\{\tilde{\psi}_{2\xi}\} = -\tilde{A}_r\Lambda_0(\bar{y}) - \left(\frac{\sigma}{\varepsilon}\right)\tilde{A}_\xi\Pi_0(\bar{y}) - \tilde{A}\tilde{A}_\xi\Omega_0(\bar{y}), \quad (2.16)$$

where

$$\Lambda_0(\bar{y}) = 2\phi'' - \frac{U''}{U-c_0}\phi, \quad (2.17)$$

$$\Pi_0(\bar{y}) = [\tilde{\rho}_0(U-c_0)\phi']' - [\tilde{\rho}_0U'\phi]', \quad (2.18)$$

and

$$\Omega_0(\bar{y}) = (\phi'^2)' - (\phi\phi'')' + \frac{1}{U-c_0} \left[\frac{r}{U-c_0}\phi \right]' \phi - \frac{r}{(U-c_0)^2}\phi\phi'. \quad (2.19)$$

Multiplying (2.16) by $[1/(U-c_0)]\phi$ and integrating to the edges of the inner region, which are $\pm\infty$ in terms of the inner variable \bar{y} , one obtains

$$\begin{aligned} \bar{A}_\tau \int_{-\infty}^{\infty} \frac{\phi}{U-c_0} \Lambda_0 d\bar{y} + \left(\frac{\sigma}{\epsilon}\right) \bar{A}_\xi \int_{-\infty}^{\infty} \frac{\phi}{U-c_0} \Pi_0 d\bar{y} + \bar{A} \bar{A}_\xi \int_{-\infty}^{\infty} \frac{\phi}{U-c_0} \Omega_0 d\bar{y} \\ = -\phi \bar{\psi}_{2\xi\bar{y}} \Big|_{-\infty}^{\infty}. \end{aligned} \quad (2.20)$$

The quantity $\bar{\psi}_{2\xi\bar{y}} \Big|_{-\infty}^{\infty}$ on the right hand side of (2.20) is to be obtained by matching to the outer solutions. For the case where the density and velocity variations outside the pycnocline are weak—specifically,

$$\frac{1}{\rho_0} \frac{\rho_{0y}}{\Delta\rho/H} < O(\epsilon), \quad \frac{U_{0yy}}{U_R/H^2} < O(\epsilon)$$

—the outer region becomes a potential flow region to first order. That is, if we let $\bar{\psi}_1$ denote the first order outer solution in an expansion

$$\bar{\psi} \rightarrow \bar{\psi}(\xi, \bar{y}, \tau) = \bar{\psi}_1 + \epsilon \bar{\psi}_2 + \epsilon^2 \bar{\psi}_3 + \dots,$$

where $\bar{y}=y/H$ is the outer variable, the governing equation for $\bar{\psi}_1$ is

$$\left(\frac{H}{l}\right)^2 \frac{\partial^2}{\partial \xi^2} \bar{\psi}_1 + \frac{\partial^2}{\partial \bar{y}^2} \bar{\psi}_1 = 0$$

subject to the matching conditions

$$\lim_{\bar{y} \rightarrow \infty} \bar{\psi} = \lim_{\bar{y} \rightarrow 0^+} \bar{\psi} \quad \text{and} \quad \lim_{\bar{y} \rightarrow -\infty} \bar{\psi} = \lim_{\bar{y} \rightarrow 0^-} \bar{\psi}.$$

Since

$$\lim_{\bar{y} \rightarrow \pm\infty} \bar{\psi}_2(\xi, \bar{y}, \tau) = \frac{h/H}{\epsilon} \bar{y} \bar{\psi}_{1\bar{y}}(\xi, 0^\pm, \tau) + \bar{\psi}_2(\xi, 0^\pm, \tau),$$

one has

$$\lim_{\bar{y} \rightarrow \pm\infty} \bar{\psi}_{2\bar{y}\xi} = \frac{h/H}{\epsilon} \bar{\psi}_{1\bar{y}\xi}(\xi, 0^\pm, \tau),$$

which gives, after solving the potential flow problem,

$$\begin{aligned} \phi \bar{\psi}_{2\xi\bar{y}} \Big|_{-\infty}^{\infty} &= -\frac{\mu}{\varepsilon} \phi^2(\infty) \left[\frac{l}{H_1} + \frac{\phi^2(-\infty)}{\phi^2(\infty)} \frac{l}{H_2} \right] \bar{A}_{\xi} \\ &\quad - \frac{\mu}{\varepsilon} \phi^2(\infty) \frac{\partial^2}{\partial \xi^2} \int_{-\infty}^{\infty} \bar{A}(\xi_1, \tau) G_0(\xi - \xi_1) d\xi_1, \\ G_0(\xi) &= \left[\frac{l}{2H_1} \left\{ \coth\left(\frac{\pi}{2H_1} l\xi\right) - \operatorname{sgn}(\xi) \right\} \right. \\ &\quad \left. + \frac{\phi(-\infty)^2}{\phi(\infty)^2} \frac{l}{2H_2} \left\{ \coth\left(\frac{\pi}{2H_2} l\xi\right) - \operatorname{sgn}(\xi) \right\} \right]. \end{aligned}$$

The depth of fluid above the pycnocline has been denoted by H_1 , while that below the pycnocline is H_2 .

Therefore, the nonlinear evolution equation is found to be

$$\begin{aligned} \bar{A}_{\tau} \int_{-\infty}^{\infty} \frac{\phi}{U-c_0} \Lambda_0 d\bar{y} + \left\{ \frac{\sigma}{\varepsilon} \int_{-\infty}^{\infty} \frac{\phi}{U-c_0} \Pi_0 d\bar{y} - \frac{\mu}{\varepsilon} \phi^2(\infty) \left[\frac{l}{H_1} + \frac{\phi(-\infty)^2}{\phi(\infty)^2} \frac{l}{H_2} \right] \right\} \bar{A}_{\xi} \\ + \bar{A} \bar{A}_{\xi} \int_{-\infty}^{\infty} \frac{\phi}{U-c_0} \Omega_0 d\bar{y} - \frac{\mu}{\varepsilon} \phi(\infty)^2 \frac{\partial^2}{\partial \xi^2} \int_{-\infty}^{\infty} d\xi_1 G_0(\xi - \xi_1) \bar{A}(\xi_1, \tau) = 0. \quad (2.21) \end{aligned}$$

In terms of the dimensional amplitude

$$A(x, t) = \varepsilon h U_R \bar{A}(\xi, \tau) = a U_R \bar{A}(\xi, \tau),$$

Equation (2.21) can be put into the following dimensional form:

$$A_t + (c + \Delta + \alpha A) A_x - \beta \frac{\partial^2}{\partial x^2} \int_{-\infty}^{\infty} G(x - x_1) A(x_1, t) dx_1 = 0, \quad (2.22)$$

where $c \equiv c_0 U_R$ is the dimensional linear Boussinesq phase speed,

$$\begin{aligned} \Delta &\equiv U_R \frac{\Delta \rho}{\rho_R} \int_{-\infty}^{\infty} \frac{\phi}{U-c_0} \Pi_0 d\bar{y} / K \\ &= \frac{\int_{-\infty}^{\infty} \frac{1}{c-u_0} \left(\phi' - \frac{u'_0}{u_0-c} \phi \right)^2 \frac{\rho_0 - \rho_0(\infty)}{\rho_0(\infty)} d\bar{y}}{2 \int_{-\infty}^{\infty} \frac{1}{c-u_0} \left(\phi' - \frac{u'_0}{u_0-c} \phi \right)^2 d\bar{y}} \quad (2.23) \end{aligned}$$

is the modification to the phase speed due to a small non-Boussinesq effect,

$$K \equiv \int_{-\infty}^{\infty} \frac{\phi}{U-c_0} \Delta_0 d\bar{y} = 2 \int_{-\infty}^{\infty} \frac{1}{c_0-U} \left(\phi' - \frac{U'}{U-c_0} \phi \right)^2 d\bar{y}, \quad (2.24)$$

$$\begin{aligned} \alpha &\equiv \frac{1}{h} \int_{-\infty}^{\infty} \frac{\phi}{U-c_0} \Omega_0 d\bar{y} / K = \frac{3}{h} \int_{-\infty}^{\infty} \frac{1}{c_0-U} \left(\phi' - \phi \frac{U'}{U-c_0} \right)^3 d\bar{y} / K \\ &= \frac{3 \int_{-\infty}^{\infty} \frac{1}{c-u_0} \left(\phi' - \frac{u'_0}{u_0-c} \phi \right)^3 d\bar{y}}{2h \int_{-\infty}^{\infty} \frac{1}{c-u_0} \left(\phi' - \frac{u'_0}{u_0-c} \phi \right)^2 d\bar{y}}, \end{aligned} \quad (2.25)$$

$$\beta \equiv \frac{U_R \phi(\infty)^2}{K} = \frac{\phi(\infty)^2}{2 \int_{-\infty}^{\infty} \frac{1}{c-u_0} \left(\phi' - \frac{u'_0}{u_0-c} \phi \right)^2 d\bar{y}}, \quad (2.26)$$

and

$$G(x) \equiv h \left[\frac{1}{2H_1} \coth \left(\frac{\pi x}{2H_1} \right) + \frac{\phi(-\infty)^2}{\phi(\infty)^2} \frac{1}{2H_2} \coth \left(\frac{\pi x}{2H_2} \right) \right]. \quad (2.27)$$

Equation (2.22) has the same form as the corresponding equation for the shearless case, but the coefficients are in general different. It is easily seen that the coefficients in the present case reduce to those of Kubota, Ko, and Dobbs [17] when the shear is allowed to approach zero; i.e.,

$$\alpha \rightarrow \frac{3}{2h} \int_{-\infty}^{\infty} \phi'^3 d\bar{y} / \int_{-\infty}^{\infty} \phi'^2 d\bar{y}, \quad (2.28)$$

$$\beta \rightarrow \frac{c}{2} \phi^2(\infty) / \int_{-\infty}^{\infty} \phi'^2 d\bar{y}, \quad (2.29)$$

$$\Delta \rightarrow -\frac{c}{2} \left(\frac{c}{U_R} \right) \int_{-\infty}^{\infty} \left(\frac{\rho_0 - \rho_R}{\rho_R} \right) \phi'^2 d\bar{y} / \int_{-\infty}^{\infty} \phi'^2 d\bar{y} \quad (2.30)$$

as $U' \rightarrow 0$. (Also, $U \rightarrow 0$, or c is measured with respect to the background current U .)

It is also easy to show that our equation (2.22) for finite depth reduces to the KdV equation when the depth of the fluid is small compared to the wavelength, and to the Benjamin-Ono equation when the fluid depth is large compared to the wavelength. In other words, Equation (2.22) contains the abovementioned equations as special cases. This has been demonstrated in Kubota, Ko, and Dobbs [17], and since the procedure used there is not affected by the presence of shear, we shall not repeat it here.

3. Nonlinear viscous critical layers

The existence of solitonlike solutions to the evolution equation for the shearless case has been demonstrated numerically by Kubota, Ko, and Dobbs [17], and analytically by Joseph [15] for a special case. Since Equation (2.22) has the same form as the equation in the shearless case, solitary waves can also be shown to exist in the presence of shear. The fact that waves of permanent form can exist in the presence of available shear energy suggests that there is probably no energetic interaction between the waves and the shear flow. A result is derived in Appendix A establishing the noninteraction of weakly nonlinear waves and the mean flow in the absence of critical levels. The question concerning the possibility of interactions in the presence of critical levels will be discussed here.

The presence of a singularity at the critical level is an indication that the linear inviscid equations are not capable of adequately describing the physical system near where $U - c_0 = 0$. Other physical mechanisms, such as viscosity and nonlinearity, have to be taken into account in a thin layer (called the critical layer) close to where $U - c_0 = 0$.

The degree to which an internal wave can energetically interact with the mean flow depends crucially on the relative magnitudes of the viscosity and nonlinearity. For unstratified shear flows, Haberman [12] showed that the ratio of viscosity to nonlinearity is quantitatively characterized by a single parameter λ_c , given in his notation by

$$\lambda_c = \frac{|U'_c|^{1/2}}{kR(\epsilon B)^{3/2}}. \quad (3.1)$$

In his problem, $k\epsilon B U_R$ is a measure of the typical vertical velocity V . k is the wavelength made dimensionless by some typical vertical scale, which is h in our problem. U'_c is the dimensionless shear at the critical level and so is the same as our U'_y evaluated at $\bar{y} = \bar{y}_c$. R is a Reynolds number involving the typical velocity U_R and typical vertical scale h so that

$$R = \frac{U_R h}{\nu}$$

with ν being the kinematic viscosity.

It is easy to show that Equation (3.1) can be put into the following more physical form:

$$\lambda_c = \frac{(\text{Re})_{\text{shear}}^{-1}}{(V/U_R)^{3/2}}, \quad (3.2)$$

where $(\text{Re})_{\text{shear}} = U_R L/\nu$ is the Reynolds number based on a shear length scale defined by

$$L = l^{1/2} \left| \frac{u_{0y}}{U_R} \right|^{-1/2} \quad (3.3)$$

In Equation (3.3) u_{0y} is the (dimensional) shear at the critical level. Equation (3.2) clearly shows that λ_c is a measure of the ratio of the viscosity, measured by $(\text{Re})_{\text{shear}}^{-1}$, and the nonlinearity, measured by $(V/U_R)^{3/2}$.

For a stratified medium, one can deduce from the work⁴ of Maslowe [20] that Equation (3.1) should be modified to

$$\lambda_c = \frac{(\text{Re})_{\text{shear}}^{-1}}{(V/U_R)^{3q}}, \quad (3.4)$$

where

$$q = \begin{cases} 1/\left\{\frac{3}{2} + \left(\frac{1}{4} - \text{Ri}\right)^{1/2}\right\} & \text{for } \text{Ri} < \frac{1}{4}, \\ \frac{2}{3} & \text{for } \text{Ri} \geq \frac{1}{4}. \end{cases}$$

Here Ri is the local Richardson number, defined as the ratio of the square of the Brunt-Väisälä frequency divided by the shear, i.e.,

$$\text{Ri} \equiv \frac{N^2}{u_{0y}^2} \Big|_{y=y_c}$$

For $\text{Ri}=0$, (3.4) reduces to (3.1) for the unstratified fluid. q increases as the stratification becomes stronger and reaches a maximum value of $\frac{2}{3}$ for $\text{Ri} \geq \frac{1}{4}$. Therefore, λ_c can at most be altered from (3.1) to

$$\lambda_c = \frac{1/(\text{Re})_{\text{shear}}}{(V/U_R)^2} \quad \text{for } \text{Ri} \geq \frac{1}{4}. \quad (3.5)$$

⁴Note that a corresponding study for stratified flows of the phase shift as a function of intermediate values of λ_c is not yet available in the literature. Only the results for very large or very small values of λ_c are known.

In our problem, the quantity U_R is of the order of the linear phase speed of the internal wave in the pycnocline and usually has the magnitude of

$$U_R \sim 0.5 \text{ m/sec.}$$

A typical value for shear in the ocean is about

$$u_{0,y} \sim 1 \text{ cm/sec per 10 m,}$$

so

$$|U_R/u_{0,y}| \sim 500 \text{ m.}$$

If the value $\nu \sim 0.01 \text{ cm}^2/\text{sec}$ for the molecular viscosity of water is used, the relevant Reynolds number is

$$(\text{Re})_{\text{shear}} \sim \left(\frac{l}{100 \text{ m}} \right)^{1/2} \times 10^8.$$

Thus, for a 100-m wave, it is 10^8 , and it becomes even larger for longer waves. The nonlinearity parameter V/U_R is a direct function of the amplitude of the wave under consideration. A wave displacement of the order of a couple of meters, when multiplied by the frequency of oscillation (\sim Brunt-Väisälä frequency $\sim 0.01/\text{sec}$), translates into a velocity

$$V \sim 2 \text{ cm/sec.}$$

Therefore, we have from Equation (3.1)

$$\lambda_c \sim \left(\frac{100 \text{ m}}{l} \right)^{1/2} \times 10^{-6} \quad \text{for unstratified fluid} \quad (3.6)$$

and, at most,

$$\lambda_c \sim \left(\frac{100 \text{ m}}{l} \right)^{1/2} \times 10^{-5} \quad \text{for stratified fluid,} \quad (3.7)$$

using Equation (3.5). These numbers are extremely small for most wavelengths of interest, and imply that the critical layers for waves of interest should most likely be dominated by nonlinearity. Applying Haberman's result on phase shifts across the critical level then gives a phase shift $\sim -10^{-6}$ for $l \sim 100 \text{ m}$; as compared to $-\pi$ for the viscous critical layers (see [19]).

The above scale estimate suggests that the behavior of interest near the critical level should be more akin to that predicted by Benney and Bergeron [5] and

Maslowe [20] for a nonlinear critical layer than to that of the conventional wave absorption result of Booker and Bretherton [6] based on the assumption of a viscosity dominated critical layer.

As both the wave parameters and environmental conditions vary over a considerable range, caution should be exercised in drawing a general conclusion from the above estimates. In the following, the range of validity of our result in (3.6) and (3.7) is examined by varying each parameter independently.

(1) *Wave amplitude:* To see whether the predominance of nonlinearity is a result of the moderately large wave amplitude used in the estimate, the effect of lowering the wave amplitude is now examined. For a wave amplitude that is one-tenth of the one used, we have

$$\lambda_c \sim \left(\frac{100 \text{ m}}{l} \right)^{1/2} \times 10^{-5}$$

for an unstratified fluid, and at most

$$\lambda_c \sim \left(\frac{100 \text{ m}}{l} \right)^{1/2} \times 10^{-3}$$

for a stratified one. Both numbers are still much less than one for most wavelengths.

(2) *Viscosity due to turbulence:* The value of ν used to arrive at the estimation (3.6) and (3.7) is based on the laminar molecular viscosity of water; the presence of turbulence near the critical layer should alter the result somewhat by changing the effective "viscosity." Though there is no general agreement as to the magnitude of turbulence in the ocean, an eddy viscosity as high as

$$\nu \sim 10^3 \text{ cm}^2/\text{sec},$$

a value five orders of magnitude larger than the one used, has sometimes been used to model that turbulence (see, e.g., [18]). This value would change the estimates in (3.6) to

$$\lambda_c \sim \left(\frac{100 \text{ m}}{l} \right)^{1/2} \times 10^{-1}$$

and (3.7) to

$$\lambda_c \sim \left(\frac{100 \text{ m}}{l} \right)^{1/2}.$$

These numbers are on the borderline for viscous effects to be felt by the wave.

Thus we see that, unless a very large eddy viscosity is used for turbulent flows, the effect of viscosity is usually not as important as the effect of nonlinearity in the critical layer for most waves under normal oceanic conditions. If the transient behavior of the waves can be ignored, our result seems to indicate that there is very little energy (and momentum) exchange between the wave and the shear, even in the presence of critical levels. The equation governing the evolution of weakly nonlinear long internal waves should still be Equation (2.22) with or without critical levels, because under the present situation neutral normal mode solutions exist to the Taylor-Goldstein equation (2.15) even when a critical level is present.

4. Effects of shear on wave form and wave speed: kinematic effects

4.1. No critical layer

Although, in most cases, the wave and mean flow have little dynamic interaction, the wave is significantly affected by the shear kinematically. Both the waveform and the wave speed of various modes are modified by the presence of the shear. These effects will be discussed in this section.

The waveform $\phi(\tilde{y})$ and wave speed c_0 of a weakly nonlinear wave are determinable from the linear equations. We consider the Taylor-Goldstein equation (2.15):

$$\frac{d^2}{d\tilde{y}^2}\phi + \left[\frac{\bar{N}^2}{(U-c_0)^2} - \frac{U_{\tilde{y}\tilde{y}}}{U-c_0} \right] \phi = 0, \quad \bar{N}^2 \equiv r, \quad (4.1)$$

and appropriate boundary conditions. For finite depth fluid, the "boundary conditions" applicable to the inner solutions are to be determined by matching to the outer solutions as $\tilde{y} \rightarrow \pm \infty$. On the other hand, if the total depth H is small compared to the wavelength and h/H is of order 1, then the "inner" equations are applicable over the whole depth of the fluid and boundary conditions can be applied to the inner variables:

$$\phi = 0 \quad \text{at} \quad \tilde{y} = \tilde{H}_1 \quad \text{and} \quad -\tilde{H}_2. \quad (4.2)$$

No "outer" regions exist for this case.

For the purpose of elucidating the effects of shear on the eigenfunctions and eigenvalues of (4.1), we shall first consider a simple system for which explicit analytical solutions can be found. We pick the system (4.2) and (4.1) with the assumption $U_{\tilde{y}\tilde{y}} = 0$ and $\bar{N} = \text{constant}$ in $-\tilde{H}_2 \leq \tilde{y} \leq \tilde{H}_1$. Note that the second assumption is not applicable for the finite depth fluid. A variable N , general depth case will be treated later numerically.

For comparison, we first consider the case with no shear by setting $U=0$. The solutions to

$$\frac{d^2}{d\bar{y}^2}\phi + \frac{\bar{N}^2}{c_0^2}\phi = 0,$$

$$\phi = 0 \quad \text{at} \quad \bar{y} = \bar{H}_1 \quad \text{and} \quad -\bar{H}_2$$

are

$$\phi = \phi_n = \sin\left[\frac{\bar{N}}{c_{0,n}}(\bar{y} + \bar{H}_2)\right], \quad (4.3)$$

$$c_{0,n} = \pm \frac{\bar{N}\bar{H}}{n\pi}, \quad n = 1, 2, 3, \dots, \quad (4.4)$$

where $\bar{H} = \bar{H}_1 + \bar{H}_2 = H/h$. n is called the mode number, and $n-1$ is the number of nodes in the vertical in the interior of the fluid. For example, a mode-1 wave has no nodes in the interior and is therefore either a wave of elevation or a wave of depression. Note that (4.4) implies that waves with higher mode numbers (and hence smaller scales) travel at smaller phase speeds than waves with lower mode numbers. Thus a wave with a definite waveform and the lowest possible mode number will emerge from an initial disturbance after leaving behind in its trail the higher mode projections of the original disturbance.

The simple case of uniform shear,

$$U(\bar{y}) = U'_0 \bar{y}, \quad U'_0 > 0, \quad (4.5)$$

is next considered. (4.1) becomes

$$\frac{d^2}{d\bar{y}^2}\phi + \frac{\text{Ri}}{(\bar{y} - c_0/U'_0)^2}\phi = 0,$$

$$\phi = 0 \quad \text{at} \quad \bar{y} = \bar{H}_1 \quad \text{and} \quad -\bar{H}_2, \quad (4.6)$$

where $\text{Ri} = \bar{N}^2/U_0'^2$ is the Richardson number. For $\text{Ri} > \frac{1}{4}$, which is the relevant case for oceanic environments, the solution to (4.6) can be written as

$$\phi = \phi_n = -\left(\frac{c_{0,n}}{U'_0} - \bar{y}\right)^{1/2} \sin\left[\mu \ln\left(\frac{c_{0,n}/U'_0 - \bar{y}}{c_{0,n}/U'_0 + \bar{H}_2}\right)\right] \quad (4.7)$$

and

$$c_0 = c_{0,n} = U'_0 \frac{(\bar{H}_1 + \bar{H}_2 e^{\pm n\pi/\mu})}{(1 - e^{\pm n\pi/\mu})}, \quad (4.8)$$

where $\mu \equiv \sqrt{Ri - \frac{1}{4}} > 0$. In deriving (4.8), we have assumed that no critical level exists in the domain for the modes under consideration. The cases with critical levels are considered later.

Since $e^{n\pi/\mu}$ is always greater than 1 and $e^{-n\pi/\mu}$ is always less than 1, (4.8) suggests that for each mode there is one wave moving in the positive direction and another moving in the negative direction, i.e.,

$$c_{0,n}^{(+)} = U_0' \frac{\tilde{H}_1 + \tilde{H}_2 e^{-n\pi/\mu}}{1 - e^{-n\pi/\mu}} > 0 \quad (4.9)$$

and

$$c_{0,n}^{(-)} = U_0' \frac{\tilde{H}_1 + \tilde{H}_2 e^{+n\pi/\mu}}{1 - e^{+n\pi/\mu}} < 0. \quad (4.10)$$

For the purpose of demonstrating the kinematic effects in a quantitative manner, it is instructive to evaluate the phase speeds of the first few modes. Take $H_2/H = \frac{1}{2}$; then $c_{0,n}^{(-)} = -c_{0,n}^{(+)}$, and

$$\frac{c_{0,n}^{(+)}}{U_{\max}} = \coth\left(\frac{n\pi}{2\mu}\right), \quad n = 1, 2, 3, \dots, \quad (4.11a)$$

or

$$\frac{c_{0,n}^{(+)}}{N\tilde{H}} = \frac{1}{2}(Ri)^{-1/2} \coth\left(\frac{n\pi}{2\mu}\right). \quad (4.11b)$$

The expression in Equation (4.11) has been evaluated for $n=1$ to 5 and various relevant Richardson numbers, and the results are listed in Table 1. We also include the values of the phase speeds for the shearless case as given by Equation (4.4) for comparison purposes.

Table 1
Effects of Shear on Phase Speed

n	$c_{0,n}^{(+)} / N\tilde{H}$ from (4.11)					$c_{0,n}^{(+)} / N\tilde{H}$ from (4.4)
	Ri = 5	10	50	100	200	Ri = ∞
1	0.362	0.340	0.323	0.321	0.319	0.318
2	0.250	0.207	0.169	0.164	0.162	0.159
3	0.230	0.174	0.121	0.114	0.110	0.106
4	0.225	0.164	0.099	0.090	0.085	0.080
5	0.224	0.160	0.088	0.076	0.070	0.064

It is easily shown that for large Richardson number, (4.11b) reduces to (4.4). Furthermore, for large n , Equation (4.11b) can be shown to be independent of the mode number n . These facts are reflected in Table 1, where it is shown that as Richardson number decreases (or shear increases) the differences between the phase speeds of various modes diminish. For the shearless case, there is a factor of 2 between the phase speed of mode 1 and that of mode 2. The ratio between the two mode phase speeds reduces to 1.91 for $Ri=50$, 1.64 for $Ri=10$, and 1.45 for $Ri=5$. The higher modes ($n>2$) travel at practically the same phase speeds for $Ri<10$.

It is also instructive to examine the effect of a uniform shear on the mode shape by comparing the distributions calculated from (4.4) and (4.11). Figure 1 shows the shape of a mode-1 wave for various Richardson numbers for the case of $H_1=H_2=H/2$. Since the system is homogeneous in ϕ , these expressions have been normalized to yield $\phi(0)=1.0$ for the purpose of comparison. Note that the symmetry in y , as shown for the shearless case ($Ri \rightarrow \infty$), is destroyed with the introduction of shear. The slight increase in wave speed with increasing shear can be correlated with the shift of maximum of ϕ into regions of higher background velocity. The effect of the uniform shear on the shape of a mode-2 wave ($n=2$) is more pronounced, as shown in Figure 2. Here, no attempt was made to normalize the eigenfunction. But it is easily seen that the perfect antisymmetry of the

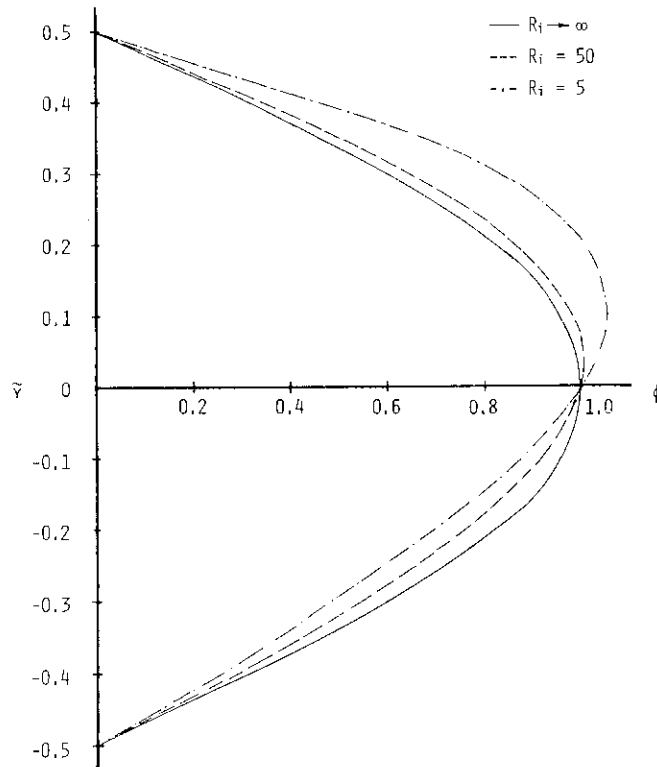


Figure 1. Effect of shear on mode 1 eigenfunction.

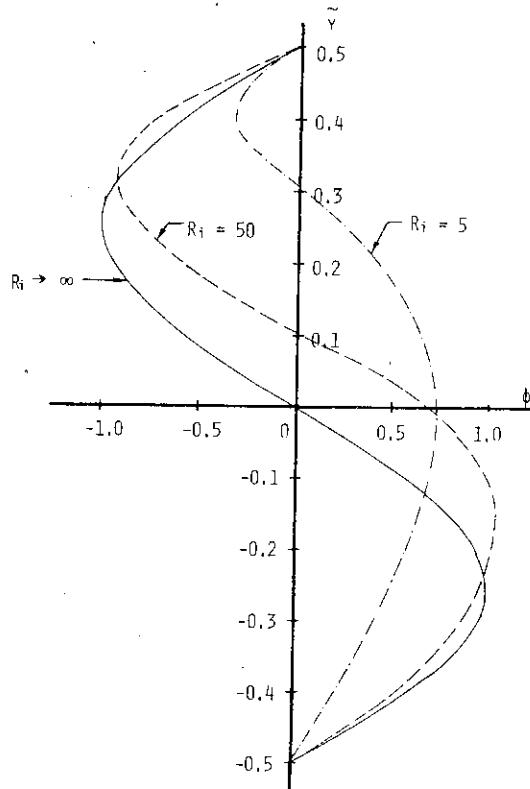


Figure 2. Effect of shear on mode 2 eigenfunction.

shearless case is lost as the Richardson number decreases. A similar observation can be made for the higher modes with an increasing degree of distortion. Figure 3 shows the effects on mode-3 ($n=3$). The fact that the higher modes under the influence of strong background shear yield a mode shape analogous to the lower mode wave's distribution over a significant flow domain may explain the increasing proximity of the speeds for various wave modes.

In addition to the modal shape change caused by the presence of a background shear, another factor could contribute to the distortions in waveform: the simultaneous presence of various modes in the case of high background shear because of the closeness in wave speeds.⁵ Therefore, when various wave modes are generated simultaneously, it will take a much longer time for the lower mode to "emerge," and the waveform will appear to be a distortion from a pure mode wave. These observations should be examined experimentally.

4.2. Critical layers

When c_0 falls within the range of $U(\tilde{y})$ in the flow domain, a critical level occurs

⁵The interactions among various modes may be significant in this case, and deserve further study.

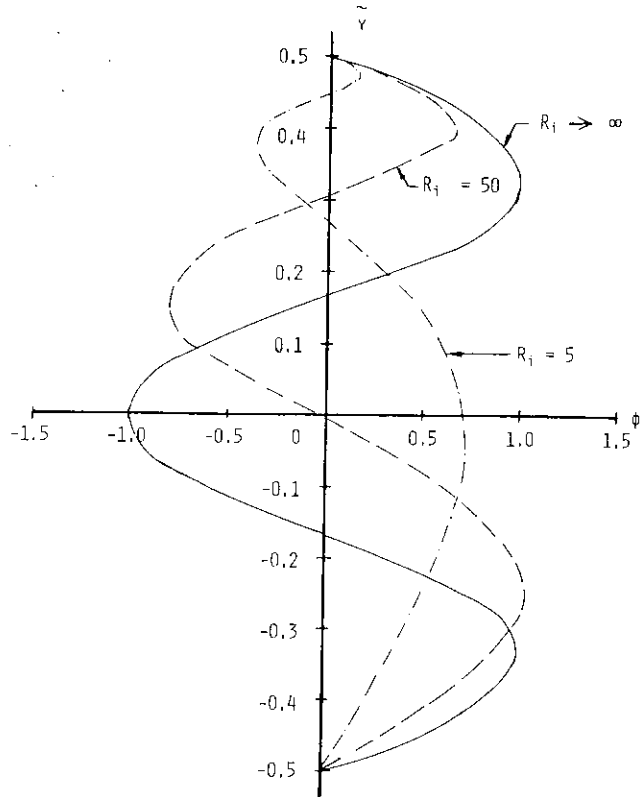


Figure 3. Effect of shear on mode 3 eigenfunction.

at

$$\bar{y} = \bar{y}_c \equiv c_0/U_0'.$$

Above the critical level, the solution that satisfies the upper boundary condition can be written, for the case $Ri > \frac{1}{4}$, as

$$\begin{aligned} \phi &= (\bar{y} - \bar{y}_c)^{1/2} \sin \left[\mu \ln \left(\frac{\bar{y} - \bar{y}_c}{\tilde{H}_1 - \bar{y}_c} \right) \right] \quad \text{for } \bar{y} > \bar{y}_c \\ &= \text{Im} \left\{ (\bar{y} - \bar{y}_c)^{1/2 + i\mu} (\tilde{H}_1 - \bar{y}_c)^{-i\mu} \right\}. \end{aligned}$$

As mentioned in the introduction, we adopt the assumption that nonlinearity is the dominant physical mechanism in the critical layer. For this case the proper continuation across the critical level is given by [21]

$$\bar{y} - \bar{y}_c \rightarrow |\bar{y} - \bar{y}_c| \quad \text{for } \bar{y} < \bar{y}_c.$$

Thus, the solution that is valid both above and below the critical level is given by

$$\begin{aligned}\phi &= \text{Im} \left\{ |\tilde{y} - \tilde{y}_c|^{1/2 + i\mu} (\tilde{H}_1 - \tilde{y}_c)^{-i\mu} \right\} \\ &= |\tilde{y} - \tilde{y}_c|^{1/2} \sin \left[\mu \ln \left(\frac{|\tilde{y} - \tilde{y}_c|}{\tilde{H}_1 - \tilde{y}_c} \right) \right].\end{aligned}\quad (4.12)$$

To satisfy the lower boundary condition, (4.12) requires the following eigenvalue condition:

$$\mu \ln \left(\frac{\tilde{y}_c + \tilde{H}_2}{\tilde{H}_1 - \tilde{y}_c} \right) = \pm m\pi,$$

giving

$$c_0 = c_{0,m} = U_0' \frac{\tilde{H}_1 e^{\pm m\pi/\mu} - \tilde{H}_2}{1 + e^{\pm m\pi/\mu}}, \quad m = 1, 2, 3, \dots \quad (4.13)$$

For the case $H_1 = H_2$ considered earlier, (4.13) becomes

$$\frac{c_{0,m}^{(+)}}{U_{\max}} = \tanh \frac{m\pi}{2\mu} \quad (4.14)$$

and

$$\frac{c_{0,m}^{(-)}}{U_{\max}} = -\tanh \frac{m\pi}{2\mu}. \quad (4.15)$$

As $m \rightarrow \infty$, $\tanh(m\pi/\mu) \rightarrow 1$, so

$$c_{0,m}^{(+)} \rightarrow U_{\max}^- \quad \text{and} \quad c_{0,m}^{(-)} \rightarrow -U_{\max} = U_{\min}^+.$$

These connect to the limiting solutions of the no critical level shear case:

$$c_{0,n}^{(+)} \rightarrow U_{\max}^+ \quad \text{and} \quad c_{0,m}^{(-)} \rightarrow U_{\min}^-.$$

For the case of small m and large μ , (4.14) and (4.15) become

$$c_{0,m}^{(\pm)} \simeq \pm U_{\max} \frac{m\pi}{2\mu} \simeq \pm \frac{\bar{N}H}{4} \frac{m\pi}{\text{Ri}}. \quad (4.16)$$

The dependence on the "mode number" is the reciprocal of that of the uniform

background flow case:

$$c_{0,n}^{(\pm)} = \pm \frac{\bar{N}\bar{H}}{n\pi},$$

and for the case of shear but no critical levels:

$$c_{0,n}^{(\pm)} \simeq \pm U_{\max} \frac{\mu}{n\pi} \simeq \pm \frac{\bar{N}\bar{H}}{n\pi}.$$

Thus it is seen that when a critical level is present the higher modes travel *faster* than the lower modes.

4.3. A numerical example

After studying an analytic solution obtained for shallow water, we now return to the finite depth case and consider the numerical solution for hyperbolic tangent density and velocity profiles, i.e.,

$$r(\tilde{y}) = r_0 \operatorname{sech}^2 \tilde{y}, \quad (4.17)$$

$$U(\tilde{y}) = U'_0 \tanh \tilde{y}.$$

The Taylor-Goldstein equation for long waves becomes

$$\frac{d^2}{d\tilde{y}^2} \phi + \left[\frac{\operatorname{Ri} \operatorname{sech}^2 \tilde{y}}{(\tanh \tilde{y} - c_0/U'_0)^2} + \frac{2 \operatorname{sech}^2 \tilde{y} \tanh \tilde{y}}{\tanh \tilde{y} - c_0/U'_0} \right] \phi = 0. \quad (4.18)$$

where

$$\operatorname{Ri} \equiv \frac{r_0}{(U'_0)^2} = \frac{r_0(\tilde{y})}{[U'(\tilde{y})]^2}$$

is the local Richardson number. Equation (4.18) is solved numerically using a shooting method. The eigenvalues c_0/U'_0 and eigenfunctions $\phi/\phi(\infty)$ are obtained for the boundary conditions

$$\lim_{\tilde{y} \rightarrow \pm \infty} \phi'(\tilde{y}) = 0. \quad (4.19)$$

Numerically, “ $\pm \infty$ ” is taken to be approximated by $\tilde{y} = \pm 50$. The code is first validated by reproducing accurately the analytic solutions of Section 4.1. For the shear case, we have avoided the numerical difficulties associated with critical levels by restricting to the case $c_0/U'_0 > 1$. Fortunately, this limited range seems

to be sufficient for our purpose of illustrating the effects of shear on wave speeds and evolution characteristics.

For the shearless case (i.e., $Ri = \infty$), the eigenvalues are known analytically to be

$$c_{0,n} = \sqrt{\frac{r_0}{n(n-1)}}, \quad n = 2, 3, 4, \dots; \quad (4.20)$$

there does not exist a mode-1 solution in the long wave limit satisfying the imposed boundary conditions. Having reproduced (4.20) numerically, the eigenvalues for some finite values of the Richardson number are calculated for modes 2 to 5 and listed in Table 2. The numerical results can be fitted very closely by a simple analytic formula:

$$\frac{c_{0,n}}{U_0'} = \sqrt{\frac{Ri}{n(n-1)} + 1}, \quad (4.21)$$

or, in a different form,

$$c_{0,n} = \sqrt{\frac{r_0}{n(n-1)} + U_0'^2}, \quad n = 2, 3, 4, \dots \quad (4.22)$$

From (4.21) it can be seen that the separation between the phase speeds of various modes decreases when the Richardson number is decreased, a conclusion already mentioned in Section 4.1. It is also seen from (4.22) that the phase speed for a fixed mode increases in the presence of shear, irrespective of the sign of shear. It may be useful at this point to comment that the preceding observation suggests that when a wave speed in excess of the linear shearless value is observed, it should not be automatically attributed to nonlinearity before the effect of shear is properly assessed.

In addition to affecting the mode structure and phase speed of an internal wave, the presence of shear can also significantly influence its nonlinear evolu-

Table 2
Phase Speeds for Various Richardson Numbers

Ri^{-1}	$c_{0,2}/U_0'$	$c_{0,3}/U_0'$	$c_{0,4}/U_0'$	$c_{0,5}/U_0'$
0.01	7.14	4.20	3.06	2.45
0.04	3.67	2.27	1.76	1.50
0.09	2.56	1.69	1.39	1.25
0.16	2.03	1.43	1.23	1.15
0.25	1.73	1.29	1.15	1.10
0.36	1.55	1.21	1.11	1.07
0.49	1.42	1.16	1.08	1.05

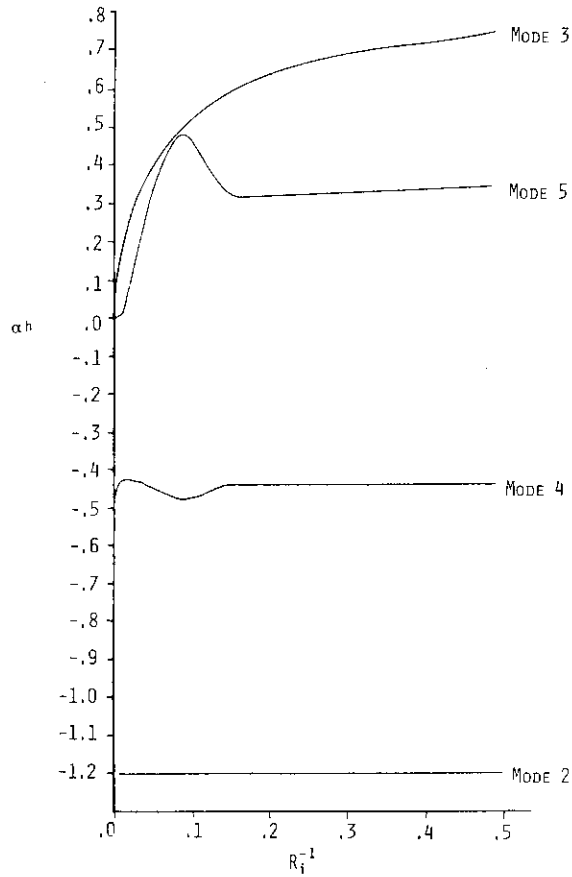


Figure 4. The variation of the nonlinear parameter α as a function of shear (Ri^{-1}).

tion. This effect comes about through modifications by shear of the coefficients α , β , etc., in the nonlinear evolution equation (2.22). The variation of α as a function of Ri^{-1} is depicted in Figure 4 for modes 2–5, while the behavior of β is plotted in Figure 5. For mode 2, α is not affected by the presence of shear, but β is decreased. This fact seems to suggest that for mode 2 shear affects only the dispersiveness of the wave. However, it can be inferred from the numerical results that the quantity

$$\beta c_0$$

is independent of the Richardson number for a fixed mode. For the case where the initial condition to the evolution equation (2.22) is a solitary wave solution for $Ri^{-1}=0$, the evolution of this wave in the presence of shear (i.e., with α and β determined for $Ri^{-1} \neq 0$) is, except for a faster phase speed, the same as in the shearless case, namely, the initial solitary wave shape remains unchanged in time, as can be seen in Figures 6 and 7.

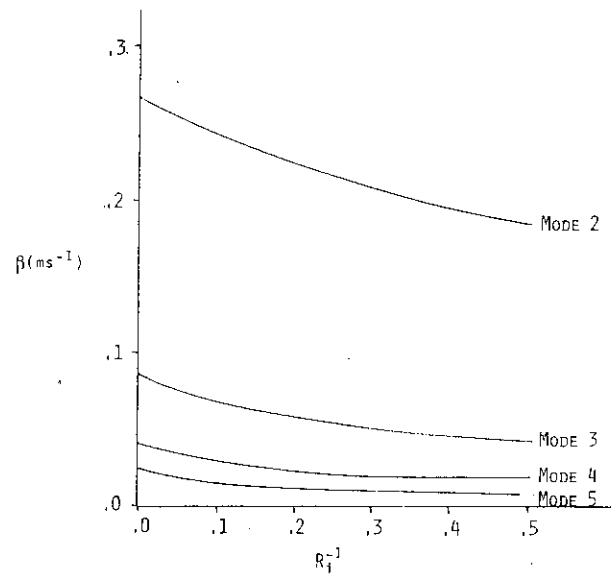


Figure 5. The variation of the dispersion parameter β as a function of shear (Ri^{-1}).

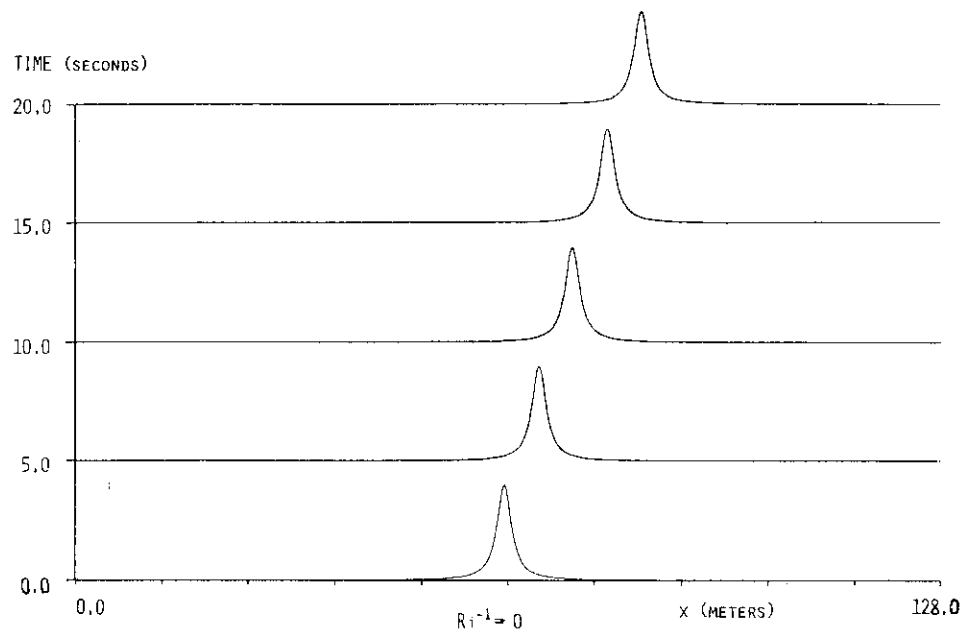


Figure 6. The time evolution of an initial solitary wavelshape in the absence of shear. Pycnocline assumed to be in the middle of a fluid of 200 m depth.

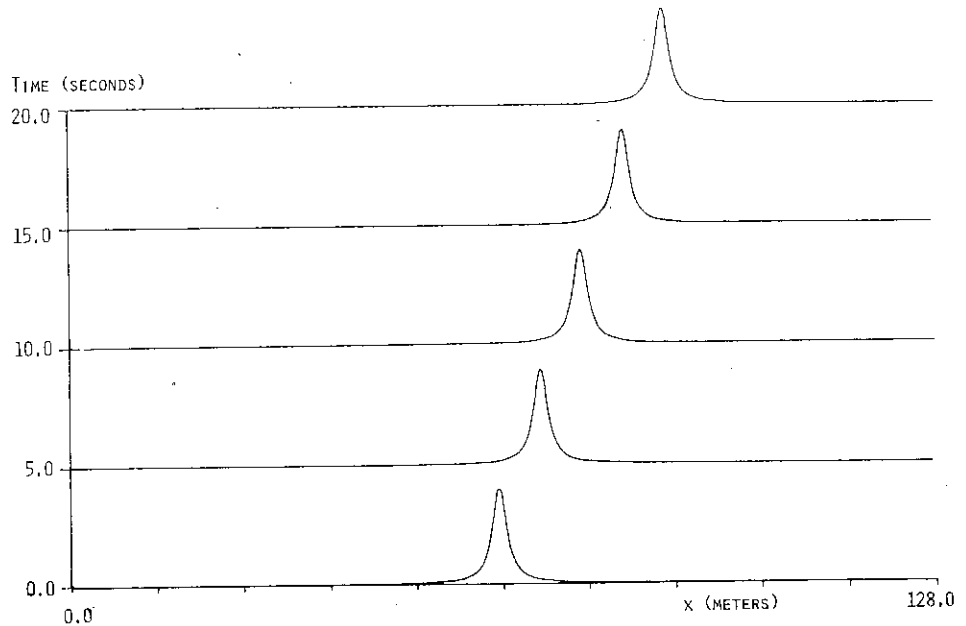


Figure 7. The evolution of an initial solitary waveform from Figure 6 in a sheared medium. α and β are calculated for mode 2 and $Ri^{-1} = 0.36$.

Figure 6 depicts the evolution of a *solitary wave* solution for $Ri^{-1} = 0$ (i.e., no shear), and in Figure 7 the time evolution of the same initial wave shape in a sheared medium with $Ri^{-1} = 0.36$ is shown. The waveshape remains unchanged for this case even when β changes because the solitary wave solution to Equation (2.22) is determined by the parameters α and βc_0 only (see [15]), which are found to be unchanged by the presence of shear.

The nonlinear evolution of a mode-3 wave is different from the behavior described above. As can be seen in Figure 4, the α for mode 3 increases quite dramatically with increasing shear magnitude. In the absence of shear (i.e., $Ri^{-1} = 0$), α is zero for mode 3, and so no solitary wave exists to the order of weak nonlinearity retained in this study. The nonlinear parameter α becomes positive in the presence of shear, and consequently positive solitary waves [with $A > 0$ in Equation (2.22)] can exist. Figure 8 depicts one such solitary wave solution to Equation (2.22) for $Ri^{-1} = 0.01$. In Figure 9, we show the evolution of the same wave in a medium with a stronger shear ($Ri^{-1} = 0.36$) and hence a larger value of α from Figure 4. It is seen that the wave steepens in time, and eventually appears to break down into two solitary waves.

5. Conclusion

The kinematic and dynamic effects of vertical shear on the propagation and evolution of weakly nonlinear long internal waves in a stratified medium of finite depth have been investigated. In the absence of critical levels, the wave does not exchange energy or momentum with the background flow, and therefore the

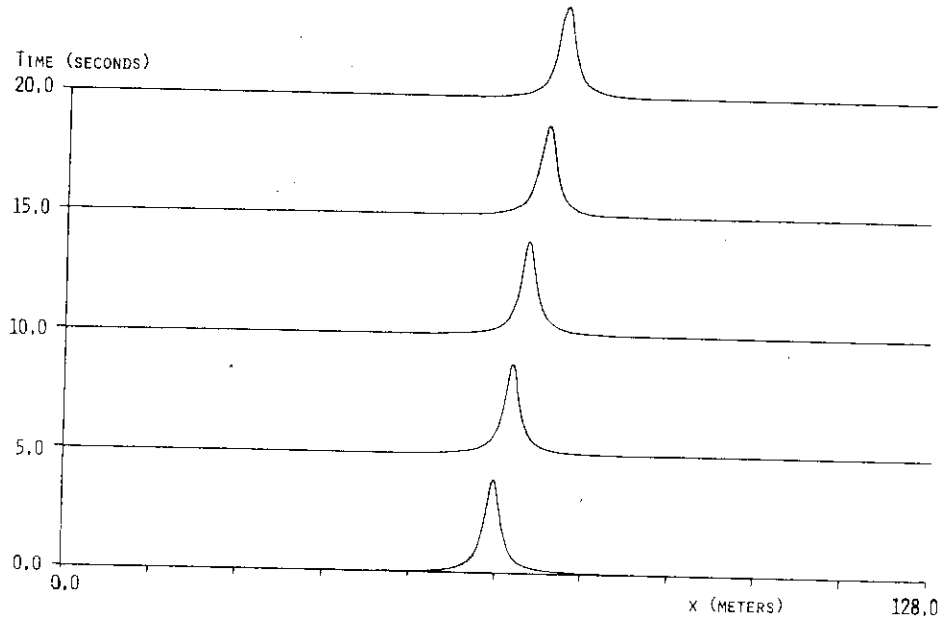


Figure 8. Solitary wave solution for mode 3 and $Ri^{-1}=0.01$. In this calculation, the pycnocline is located in the middle of a 200 m depth fluid.

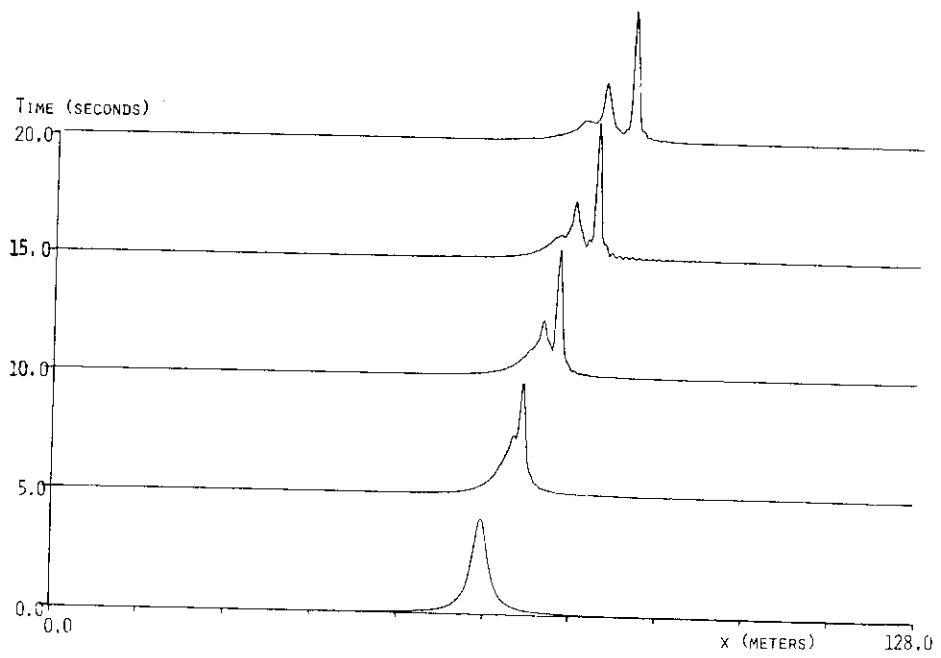


Figure 9. The evolution of the waveform in Figure 8 in a medium with $Ri^{-1}=0.36$.

effects of the shear are mostly kinematic: i.e., changes in wave speed and waveform. The nonlinear evolution of the wave, however, is greatly affected by the presence of the shear through the changes in the coefficients in the evolution equation. When critical levels are present in the domain, the possibility exists that wave-mean-flow interaction may take place, which would then prevent the formation of waves of permanent form. However, for long waves under oceanic conditions, it is found that the critical layer is dominated by nonlinearity instead of viscosity (the Benney-Bergeron limit), and as a consequence, almost no energetic interaction takes place between the wave and the mean flow if it is assumed that the critical layer can reach a steady state. The effects of shear on the internal wave are again kinematic.

Appendix A. A noninteraction theorem

In this appendix, we seek to prove that the mean flow energy is not increased or decreased in the presence of wave energy and momentum fluxes to second order in the wave amplitude. The noninteraction result then clearly follows. This result is similar to the theorem of Eliassen and Palm, and seems to be true for a more general class of fluid systems [1, 2, 7, 9]. Since we are specifically interested in the effects of shear, the effects due to density stratification will be ignored, and the Boussinesq approximation is used in the discussion to follow.

The horizontal momentum equation is

$$\rho_0 \left[\frac{\partial}{\partial t} u + u \frac{\partial}{\partial x} u + v \frac{\partial}{\partial y} u \right] = - \frac{\partial}{\partial x} p. \quad (\text{A.1})$$

The background flow for a weakly nonlinear case is defined as the horizontal average of the flow field, i.e.,

$$U = \bar{u} \equiv \lim_{L \rightarrow \infty} \frac{1}{2L} \int_{-L}^L u dx. \quad (\text{A.2})$$

We let the deviation from the background flow be small, i.e.,

$$\begin{aligned} u' \equiv \frac{u - \bar{u}}{\epsilon} = O(1), \quad \text{or} \quad u = \bar{u} + \epsilon u' + O(\epsilon^2), \\ v' \equiv \frac{v}{\epsilon} = O(1), \quad \text{or} \quad v = \epsilon v' + O(\epsilon^2). \end{aligned} \quad (\text{A.3})$$

U , as defined by (A.2), is independent of x , but is a function of t and y . We restrict our analysis to slowly varying background flow, which is equivalent to the assumption that U does not change with time to order ϵ , i.e., U is independent of ξ and τ . Thus U can change only in a time scale

$$t = O(\epsilon^{-2}),$$

so we let $T = \varepsilon^2 t$. This assumption is consistent with our purpose of investigating the changes in the mean flow in response to the Reynolds stress of the wave momentum, a quantity which is of the order of ε^2 .

Thus, averaging Equation (A.1) according to (A.2) and retaining the order ε^2 terms, we have

$$\frac{\partial}{\partial T} \bar{u} = - \frac{\partial}{\partial y} \overline{u'v'}. \quad (\text{A.4})$$

Equation (A.4) implies that the mean flow would change if there were a momentum flux convergence due to the wave. The wave field, which is of order ε , is obtainable from a linear calculation. Not restricting ourselves to the case of thin pycnoclines and long waves, we write the solution in the form

$$\begin{aligned} u' &= \text{Re } \psi_y, \\ v' &= -\text{Re } \psi_x, \\ \psi &= \Phi(y) e^{ik(x - c_0 t)}, \end{aligned} \quad (\text{A.5})$$

where k is the wave number of the wave and Φ can be complex. Thus

$$\overline{u'v'} = \frac{k}{2} [\text{Re } \Phi_y \text{Im } \Phi - \text{Re } \Phi \text{Im } \Phi_y], \quad (\text{A.6})$$

Now Φ satisfies the Taylor-Goldstein equation:

$$\frac{d^2}{dy^2} \Phi + \left[\frac{r}{(U - c_0)^2} - \frac{U''}{U - c_0} - k^2 \right] \Phi = 0, \quad (\text{A.7})$$

which is in a self-adjoint form. Applying Abel's identity for a second order self-adjoint differential equation, we note that the Wronskian

$$W \equiv \Phi^* \frac{d}{dy} \Phi - \Phi \frac{d}{dy} \Phi^*$$

is an invariant of the equation except possibly near its singularities; i.e.,

$$\frac{d}{dy} W = 0 \quad \text{when } U - c_0 \neq 0.$$

However,

$$\begin{aligned} W &= -2i [\text{Re } \Phi_y \text{Im } \Phi - \text{Re } \Phi \text{Im } \Phi_y] \\ &= -\frac{4i}{k} \overline{u'v'}. \end{aligned}$$

We thus conclude that $\overline{u'v'}$ is an invariant; i.e.,

$$\frac{d}{dy} \overline{u'v'} = 0 \quad \text{when} \quad U - c_0 \neq 0. \quad (\text{A.8})$$

This formula was first derived by Eliassen and Palm [11]. Substituting (A.8) into (A.4), we then have the desired result:

$$\frac{\partial}{\partial T} \bar{u} = 0. \quad (\text{A.9})$$

That is, the background flow does not change and hence does not interact with the wave in the absence of critical levels.

When critical levels exist in the flow domain, the noninteraction theorem breaks down where

$$u - c_0 = 0.$$

Near these regions (called critical layers), interaction between the wave and the background flow is possible, especially when viscosity is the dominant process in the critical layer. This situation is investigated in Section 4.2 of the main text.

Appendix B. Wave evolution equation for non-Boussinesq fluids

Here the Boussinesq approximation of $\sigma \equiv \Delta\rho/\rho_R = O(\epsilon) \ll 1$ used in the main text will be relaxed and the evolution equation derived for the case where $\sigma = O(1)$.

The first and second order perturbation equations, become, for $\sigma = O(1)$,

$$(U - c_0)\bar{p}_{1\xi} + r\bar{\psi}_{1\xi} = 0, \quad (\text{B.1})$$

$$\hat{\rho}_0[(U - c_0)\bar{\psi}_{1\xi\bar{y}} - U_{\bar{y}}\bar{\psi}_{1\xi}] + \bar{p}_{1\xi} = 0, \quad (\text{B.2})$$

$$\bar{p}_{1\bar{y}} + \bar{p}_1 = 0 \quad (\text{B.3})$$

and

$$(U - c_0)\bar{p}_{2\xi} + r\bar{\psi}_{2\xi} = -\bar{p}_{1\tau} - [\bar{\psi}_{1\bar{y}}\bar{p}_{1\xi} - \bar{\psi}_{1\xi}\bar{p}_{1\bar{y}}], \quad (\text{B.4})$$

$$\begin{aligned} \hat{\rho}_0[(U - c_0)\bar{\psi}_{2\xi\bar{y}} - U_{\bar{y}}\bar{\psi}_{2\xi}] + \bar{p}_{2\xi} = & -\hat{\rho}_0\bar{\psi}_{1\bar{y}\tau} - \hat{\rho}_0[\bar{\psi}_{1\bar{y}}\bar{\psi}_{1\bar{y}\xi} - \bar{\psi}_{1\xi}\bar{\psi}_{1\bar{y}\bar{y}}] \\ & - \sigma\bar{p}_1[(U - c_0)\bar{\psi}_{1\bar{y}\xi} - U_{\bar{y}}\bar{\psi}_{1\xi}] + \sigma\bar{p}_1\bar{p}_{1\xi}/\hat{\rho}_0, \end{aligned} \quad (\text{B.5})$$

$$\bar{p}_{2\bar{y}} + \bar{p}_2 = 0. \quad (\text{B.6})$$

Equations (B.1), (B.2), and (B.3) can be solved to yield

$$\bar{\psi}_1 = A(\xi, \tau)\phi(\bar{y}), \quad (\text{B.7})$$

$$\bar{\rho}_1 = -\frac{r}{U-c_0}A(\xi, \tau)\phi, \quad (\text{B.8})$$

$$\bar{p}_1 = \hat{\rho}_0[U_{\bar{y}}\phi - (U-c_0)\phi_{\bar{y}}]A(\xi, \tau), \quad (\text{B.9})$$

where ϕ now satisfies the non-Boussinesq form of the Taylor-Goldstein equation:

$$\mathcal{L}\{\phi\} = 0,$$

$$\mathcal{L} \equiv \frac{d}{d\bar{y}} \left[\hat{\rho}_0 \frac{d}{d\bar{y}} \right] + \left[\frac{r}{(U-c_0)^2} - \frac{(\hat{\rho}_0 U_{\bar{y}})_{\bar{y}}}{U-c_0} \right]. \quad (\text{B.10})$$

The second order equations (B.4), (B.5), and (B.6) can be combined to give

$$(U-c_0)\mathcal{L}\{\bar{\psi}_{2\xi}\} = -A_\tau \Lambda_1(\bar{y}) - AA_\xi \Omega_1(\bar{y}), \quad (\text{B.11})$$

where

$$\Lambda_1(\bar{y}) = 2[\hat{\rho}_0\phi']' - [\hat{\rho}_0 U']'\phi \quad (\text{B.12})$$

and

$$\begin{aligned} \Omega_1(\bar{y}) = & [\hat{\rho}_0\phi'^2]' - [\hat{\rho}_0\phi\phi'']' + \frac{\phi}{U-c_0} \left[\frac{r}{U-c_0}\phi \right]' - \frac{r}{(U-c_0)^2}\phi\phi' \\ & + \sigma \left\{ -(r\phi\phi')' + \frac{r}{U-c_0}U'\phi\phi' + 2\phi \left(\frac{r}{U-c_0}\phi U' \right)' \right. \\ & \left. - (U-c_0) \left(\frac{r}{U-c_0}\phi\phi' \right)' \right\}. \quad (\text{B.13}) \end{aligned}$$

Multiplying (B.11) by $\phi/(U-c_0)$ and integrating with respect to \bar{y} to $\pm\infty$, one obtains

$$K_1 A_\tau + K_1 \alpha_1 A A_\xi = -\hat{\rho}_0 \phi \bar{\psi}_{2\xi \bar{y}} \Big|_{-\infty}^{\infty}, \quad (\text{B.14})$$

where

$$K_1 \equiv \int_{-\infty}^{\infty} \frac{\phi}{U-c_0} \Lambda_1 d\tilde{y}, \quad (\text{B.15})$$

$$\alpha_1 \equiv \int_{-\infty}^{\infty} \frac{\phi}{U-c_0} \Omega_1 d\tilde{y} / K_1. \quad (\text{B.16})$$

Assuming the density stratification is weak in the outer region [i.e., $\bar{N}^2 < O(1)$], the right hand side of Equation (B.14) is found as before to be

$$\begin{aligned} & -\hat{\rho}_0(\infty)\phi(\infty)\tilde{\psi}_{2\xi\tilde{y}}(\infty) + \hat{\rho}_0(-\infty)\phi(-\infty)\tilde{\psi}_{2\xi\tilde{y}}(-\infty) \\ & = -\frac{\mu}{\varepsilon}\hat{\rho}_0(\infty)\phi^2(\infty)\frac{\partial^2}{\partial\xi^2}\int_{-\infty}^{\infty} d\xi_1 A(\xi_1, \tau)G_1(\xi-\xi_1), \end{aligned} \quad (\text{B.17})$$

where

$$G_1(\xi) \equiv \frac{\delta}{\mu} \left[\frac{1}{2\bar{H}_1} \coth\left(\frac{\pi\delta}{2\mu\bar{H}_1}\xi\right) + \frac{\hat{\rho}_0(-\infty)}{\hat{\rho}_0(\infty)} \frac{\phi^2(-\infty)}{\phi^2(\infty)} \frac{1}{2\bar{H}_2} \coth\left(\frac{\pi\delta}{2\mu\bar{H}_2}\xi\right) \right]. \quad (\text{B.18})$$

Therefore the evolution equation is

$$A_\tau + \alpha_1 A A_\xi - \frac{\mu}{\varepsilon} \beta_1 \frac{\partial^2}{\partial\xi^2} \int_{-\infty}^{\infty} G_1(\xi-\xi_1) A(\xi_1, \tau) d\xi_1 = 0 \quad (\text{B.19})$$

where

$$\beta_1 \equiv \hat{\rho}_0(\infty)\phi^2(\infty)/K_1. \quad (\text{B.20})$$

It is seen that the coefficient of the nonlinear term is affected by the density stratification in a strong pycnocline [$\sigma = O(1)$]; the non-Boussinesq effects cannot simply be accounted for by a change in the linear phase speed.

Acknowledgments

The approach used in the derivation of the evolution equation in the present article is a modification of the one used by Professor T. Kubota in an unpublished report for the shearless case. The numerical code used in solving the evolution equation was first developed for the paper by Kubota, Ko, and Dobbs [17]. The authors have also benefited from many conversations with Professor

Kubota. The authors are also grateful to Professor R. Joseph, who pointed out that the more cumbersome expressions for α and β appearing in an earlier manuscript can be written in the form adopted in Equations (2.25) and (2.26), which exhibits the dependence on shear more explicitly.

References

1. D. G. ANDREWS and M. E. MCINTYRE, An exact theory of nonlinear waves on a Lagrangian-Mean flow, *J. Fluid Mech.* 89:609-646 (1978).
2. D. G. ANDREWS and M. E. MCINTYRE, On wave-action and its relatives, *J. Fluid Mech.* 89:647-664 (1978).
3. M. BÉLAND, Numerical study of the nonlinear Rossby wave critical level development in a barotropic zonal flow, *J. Atmospheric Sci.* 33:2066-2078 (1976).
4. M. BÉLAND, The evolution of a nonlinear Rossby wave critical level: effects of viscosity, *J. Atmospheric Sci.* 35:1802-1815 (1978).
5. D. J. BENNEY and R. F. BERGERON, A new class of nonlinear waves in parallel flow, *Studies in Appl. Math.* 48:181-204 (1969).
6. J. R. BOOKER and F. P. BRETHERTON, The critical layer for internal gravity waves in a shear flow, *J. Fluid Mech.* 27:513-559 (1967).
7. J. BOYD, Noninteraction of waves with the zonally averaged flow on a spherical earth and the interrelationship of eddy fluxes of energy, heat and momentum, *J. Atmospheric Sci.* 33:2285-2291 (1976).
8. S. N. BROWN and K. STEWARTSON, The evolution of the critical layer of a Rossby wave: Part II, *J. Geo. Astrophys. Fluid Dyn.* 10:1-24 (1978).
9. R. E. DICKINSON, Theory of planetary wave-zonal flow interaction, *J. Atmospheric Sci.* 26:73-81 (1969).
10. P. G. DRAZIN and L. N. HOWARD, Hydrodynamic stability of parallel flow of inviscid fluid, *Advances in Appl. Mech.* 9:1-89 (1966).
11. A. N. ELIASSEN and E. PALM, On the transfer of energy in stationary mountain waves, *Geofys. Publikasjoner* 22:1-23 (1961).
12. R. HABERMAN, Critical layers in parallel flows, *Studies in Appl. Math.* LI:139-161 (1972).
13. E. L. INCE, *Ordinary Differential Equations*, Dover (1953).
14. W. L. JONES, Reflection and stability of waves in stably stratified fluids with shear flow: a numerical study, *J. Fluid Mech.* 34:609-624 (1968).
15. R. I. JOSEPH, Solitary waves in a finite depth fluid, *J. Phys. A* 10:L225-L227.
16. R. E. KELLEY and S. A. MASLOWE, The nonlinear critical layer in a slightly stratified shear flow, *Studies in Appl. Math.* XLIX:301-326 (1976).
17. T. KUBOTA, D. R. S. KO, and L. D. DOBBS, Weakly nonlinear long internal gravity waves in stratified fluid of finite depth, *J. Hydronautics* 12:157-165 (1978).
18. P. H. LEBLOND, On the damping of internal gravity waves in a continuously stratified ocean, *J. Fluid Mech.* 25:121-142 (1966).
19. C. C. LIN, *The Theory of Hydrodynamic Stability*, Cambridge U. P., New York (1955).
20. S. A. MASLOWE, The generation of clear air turbulence by nonlinear waves, *Studies in Appl. Math.* LI:1-16 (1972).
21. S. A. MASLOWE, Finite-amplitude Kelvin-Helmholtz billows, *Boundary Layer Meteorology* 5:43-52 (1973).
22. S. A. MASLOWE and L. G. REDEKOPP, Solitary waves in stratified shear flows, *Geophys. Astrophys. Fluid Dyn.* 13:185-196 (1979).
23. K. STEWARDSON, The evolution of the critical layer of a Rossby wave, *J. Geophys. Astrophys. Fluid Dyn.* 9:185-200 (1978).
24. T. WARN and H. WARN, The evolution of a nonlinear Rossby wave critical level, *Studies in Appl. Math.*, 59:37-71 (1978).

DYNAMICS TECHNOLOGY INC.

(Received December 11, 1979)